DOI: https://doi.org/10.20870/oeno-one.2025.59.2.9308

OPEN ACCESS

SPECIAL ISSUE

Application of spectral index-based contour mapping for non-destructive ripeness monitoring in water stressed *Vitis vinifera L.* (Cabernet-Sauvignon)

M. Ignacia González-Pavez[1], Samuel Ortega-Farias[1,*], Carlos Poblete-Echeverria[2], M. José Gamboa[1], Sebastián Vargas[1,3]

[1] Research and Extension Center for Irrigation and Agroclimatology (CITRA), Faculty of Agricultural Sciences, Universidad de Talca, Campus Talca, Chile
[2] South African Grape and Wine Research Institute (SAGWRI), Stellenbosch University, Private Bag X1, Matieland 7602, South Africa
[2] Centro de Investigación e Innovación de Viña Concha y Toro, RutaK-650 km 10 Pencahue, Chile

This article is an original research article published in cooperation with the 23rd GiESCO International Conference, July 21-27, 2025, hosted by the Hochschule Geisenheim University in Geisenheim, Germany.

Guest editors: Laurent Torregrosa and Susanne Tittmann.

Article number: 9308

*correspondence: sortega@utalca.cl

Associate editor: Laurent Torregrosa

Received: 15 March 2025

Accepted: 18 May 2025

Published: 28 May 2025

This article is published under the **Creative Commons licence** (CC BY 4.0).

Use of all or part of the content of this article must mention the authors, the year of publication, the title, the name of the journal, the volume, the pages and the DOI in compliance with the information given above.

ABSTRACT

Accurate and non-destructive monitoring of grape ripening is essential for optimising harvest decisions, particularly under water stress conditions. This study aims to evaluate the application of the contour map optimisation method for determining spectral indices to non-destructive monitoring of soluble solids (SS), titratable acidity (TA), and pH for grapevines (cv. Cabernet-Sauvignon) under four levels of water application. Hyperspectral reflectance data (350–2500 nm) were acquired from grape berries during two consecutive growing seasons (2019/20 and 2020/21) to identify optimal wavelength combinations using contour maps. Results indicated that the optimal spectral indices were SISS = 1600 nm/1412 nm for SS, SITA = 1617 nm/1415 nm for TA, and SIpH = 694 nm/697 nm for pH. In this case, the linear regression based on SISS, SITA, and SIpH presented a coefficient of determination of 0.82, 0.83, and 0.95, respectively. Model validation confirmed the stability of these spectral indices across different irrigation regimes, with an index of agreement of 0.94 for SS, 0.90 for TA, and 0.79 for pH. The results demonstrate that contour map optimisation could increase the robustness of spectral indices, improving their reliability across varying conditions of soil water availability. This methodology provides a viable alternative to destructive ripeness assessment techniques, offering a scalable solution for vineyard management and decision-making in precision viticulture.

KEYWORDS: ripeness, spectral indices, optimisation, contour map, *Vitis vinifera* L., water stress, GIESCO 2025

INTRODUCTION

Grapevine (*Vitis vinifera* L.) is an economically important crop worldwide, predominately cultivated in Mediterranean regions (Macedo *et al.,* 2020). In these regions, precipitation is scarce and irregularly distributed throughout the year, and heat wave events are becoming more intense and frequent due to climate change (del Pozo *et al.,* 2019). Under these climate conditions, irrigation management plays a significant role in maintaining or improving yield and berry quality (Santos *et al.,* 2020). In this context, regulated deficit irrigation (RDI) has been widely implemented to optimise water application while improving water productivity and fruit quality (Jara Rojas *et al.,* 2015; Ortega-Farias *et al.,* 2012; Wang *et al.,* 2019; Zúñiga *et al.,* 2018). Several reports have shown that RDI strategies influence the morphological, physical, and biochemical characteristics of berries. RDI tends to increase sugar and phenolic content while reducing titratable acidity and moderately raising pH levels (Gambetta *et al.,* 2020; Munitz *et al.,* 2020). Rouxinol *et al.* (2022) suggested that water deficits can increase sugar concentration by reducing dilution in smaller berries; however, this response varies and depends on grape cultivars and climatic conditions. Additionally, the rise in temperature due to climate change has induced changes in phenological progression, berry development, and maturation dynamics. These changes affect berry composition, advance the veraison date, and increase sugar concentration, leading to harvests earlier than expected. Therefore, decision-making tools are essential for monitoring the evolution of grape composition, with the goal of optimising harvest time and maintaining wine quality, according to their specific wine level and commercial strategy (Gamboa *et al.,* 2024).

The evaluation of berry ripening is typically performed using destructive methods that demand significant manual labour and skilled personnel to estimate the optimal harvest time (Manley, 2014). The non-destructive analysis of fruit maturity parameters (soluble solids, titratable acidity, and pH) provides a considerable advantage over traditional methods by preserving the sample, maintaining the fruit in its complete and intact state, and enabling repeated and continuous measurements of its chemical evolution (Daniels *et al.,* 2019; Donis-González *et al.,* 2020). Accurately and rapidly monitoring grape maturation is crucial for identifying homogeneous zones with the optimal harvest time, a process that remains difficult to predict or estimate (Basile *et al.,* 2021; Chariskou *et al.,* 2022; Ghozlen *et al.,* 2010). Thus, the need for the adoption of non-destructive technologies is becoming increasingly important and steadily growing. Research has focused on developing non-destructive spectral reflectance (SR)-based tools for monitoring the ripening process and evaluating the internal chemistry of agricultural products (Goisser *et al.,* 2021; Walsh *et al.,* 2020). Due to their non-invasive approach, the SR-based tools allow for various measurements to be made on the same fruit sample during their physiological evolution, decreasing sampling time and increasing the number of samples available, which generates more representative information in real-time, without the need to destroy the sample (Costa *et al.,* 2022; Piazzolla *et al.,* 2013). In comparison with the current maturity monitoring, SR-based tools can carry out a greater number of measurements in a shorter period and in a non-destructive way, thus generating savings both in laboratory material as well as in handwork (Cao *et al.,* 2010; Fernandes *et al.,* 2015).

Various studies have investigated the use of different wavelength ranges-visible (VIS, 400–700 nm), near-infrared (NIR, 700–1300 nm), and middle-infrared (SWIR, 1300–2500 nm)—to estimate soluble solids, titratable acidity, and pH. For example, Fernández-Novales *et al.* (2019) found strong correlations (R^2 = 0.90 to 0.98) between visible spectrum (400–700 nm) measurements and soluble solids in the cultivar Grenache. Giovenzana *et al.* (2013) reported significant relationships (R^2 = 0.7 to 0.8) between wavelengths in the VIS range (500–700 nm) and both soluble solids and titratable acidity in Cabernet-Sauvignon. Fadock *et al.* (2016) developed non-linear models using 50–850 nm wavelengths to estimate soluble solids, pH, titratable acidity, and anthocyanin content in Cabernet-Sauvignon, Cabernet franc, and Syrah, with R^2 values ranging from 0.30 to 0.90. Kemps *et al.* (2010) used wavelengths between 700–1600 nm to estimate anthocyanins in Syrah and Cabernet-Sauvignon (R^2 = 0.8–0.9) and identified wavelengths near 700 nm as effective for measuring sugar content (R^2 = 0.78–0.93). In addition, several spectral indices (SI) have been developed using wavelength ratios from the VIS, NIR, and SWIR regions to estimate pH, titratable acidity, and soluble solids. The absorbance difference index (IAD), calculated from wavelengths of 560 and 640 nm, has been correlated with soluble solids (SS) and titratable acidity (TA) with R^2 between 0.9 and 0.8, respectively (Ribera-Fonseca *et al.*, 2016). The photochemical reflectance index (PRI), calculated from wavelengths of 570 and 530 nm, and the normalised difference vegetation index (NDVI), obtained from wavelengths of 800 and 670 nm, have been evaluated for their relationship to SS, TA, pH, and other variables (Suarez *et al.*, 2021). Similarly, Gamboa *et al.* (2024) conducted a study in which they evaluated the normalised difference spectral index (NDSI29), calculated from the 420 and 720 nm wavelengths, to estimate soluble solids (SS), titratable acidity (TA), and pH. The main limitation of SI-based models is the site-specific nature of the approach. The accuracy of these models can be affected by variables such as crop type, species, fruit morphology and physiology, water content, and the atmospheric conditions of the environment in which the models were developed (Suarez *et al.*, 2021; Tardaguila *et al.*, 2021). These dependencies impact the stability and consistency of SI-based models over time, limiting their broader applicability. As a result, local calibration and optimisation of models based on SI are essential for improving their accuracy and reliability. To address these issues, the contour map methodology has been proposed as an alternative to develop more robust indexes. This approach offers a graphical representation of a correlation matrix, allowing the identification of "hot spots"

where optimal combinations of wavelengths can be found for estimating a specific variable of interest. This approach optimises the spectral resolution through an interpolation process, generating a spectral signature with a wavelength resolution at 1 nm intervals, which facilitates an exhaustive analysis to calculate and develop narrowband indices. For this purpose, the Savitzky-Golay (SG) filter can be applied to remove noise and random fluctuations in the spectral data (Pôças *et al.,* 2015; Rallo *et al.,* 2014). The contour map methodology has been applied in several agricultural studies across different ways to optimise the spectral indices described in the literature for estimating physiological variables. It has resulted in improvements in correlation coefficients through the development of new formulations for specific indices (Inoue *et al.,* 2008; Tian *et al.,* 2011; Yao *et al.,* 2010). For *Vitis vinifera* L. cv. "Touriga Nacional" the relationship between pre-dawn leaf water potential and fifteen vegetation indices was evaluated. All indices were calculated using both their standard formulations and optimised versions (spectral resolution every 1 nm). For example, the photochemical reflectance index (PRI) increased its coefficient of determination (R^2) from 0.39 to 0.82 based on a new combination of wavelengths (Pôças *et al.,* 2015).

Limited scientific research has been reported on the use of contour maps to improve the accuracy of SI-based models for monitoring grape ripeness under varying water levels. This study aims to evaluate the application of the contour map optimisation method for determining spectral indices for non-destructive monitoring of soluble solids, titratable acidity, and pH in grapevines under four levels of water application. By employing contour maps, this research aims to identify specific wavelength combinations, allowing the creation of new spectral indices with improved sensitivity and stability during growing seasons.

MATERIALS AND METHODS

1. Description of the experimental site

The study was carried out in a commercial vineyard located in the Pencahue Valley (–35,43°, –71,80°; 104 m above sea level) of the Maule Region, Chile during the 2019/20 and 2020/21 growing seasons. This valley has a temperate Mediterranean climate with an annual rainfall of 562 mm and reference evapotranspiration (ETr) of 689 mm $year^{-1}$. The grapevine growing seasons used in this study (from November to March) were dry and hot, with an average daily temperature of 21 °C and ETr value of 6.4 mm day^{-1}.

The vineyard was planted in 2014 with Cabernet-Sauvignon vines grafted on SO_4 rootstock (*Vitis berlandieri* × *Vitis riparia* Selection Oppenheim 4). Vines were trained using a vertical shoot-positioned system (VSP) oriented in a north-south direction with a plant density of 2.3 m × 1.2 m, a canopy length of 1.2 m, and pruned using the Guyot method with two canes per vine (between 7 and 8 buds per cane). Water application was carried out weekly, using two drippers per vine with a flow rate of 2.5 L h^{-1}, located 0.6 m apart from each other across the irrigation line.

2. Experimental design

The experimental design was a randomised block design (RBD), with blocking based on soil depth due to the presence of a hardpan in certain repetitions. The experiment consisted of four treatments with four replicates. Each replicate included six complete rows; however, harvested fruit was obtained exclusively from the two central rows. For the T0 and T1 treatments, water application corresponded to 100 % and 70 % of evapotranspiration (ETa) during the entire growing season, respectively. Water application for T2 was based on 50 % ETa from fruit set (FS) to veraison (V) and 100 % ETa from V to harvest (H); whilst for T3 it corresponded to 30 % ETa from FS to V, and 100 % from V to H.

3. Measurements of midday stem water potential (Ψx)

Ψx measurements were taken from two healthy, mature leaves per replicate, selected from the middle third of the canopy and exposed to sunlight. The leaves were wrapped in plastic film and aluminium foil to prevent gas exchange and light absorption. After two hours, they were detached from the branch, and Ψx was measured using a Scholander pressure chamber (model 600, PMS Instrument Company, Oregon, USA) (Fulton *et al.,* 2014; Scholander *et al.,* 1965).

4. Berry sampling

From veraison to harvest, shaded and sun-exposed clusters were randomly sampled at morning hours (7:30 to 8:30 local time). Samples from the 2019/20 season were collected from January 22 to March 12 (harvest), while those for the 2020/21 season were taken from January 27 to March 24 (harvest). Every week, two hundred berries per replicate were harvested to measure soluble solids, titratable acidity, and pH.

5. Determination of soluble solids (SS), titratable acidity (TA) and pH

The 200 berries were manually ground or pressed to extract the most homogeneous juice possible, trying to obtain only liquid without solid parts. This liquid was used for SS, TA, and pH measurements according to the standard methodologies proposed by the OIV (OIV 2025). SS was estimated using a refractometer (model Pla $^{-1}$, TW, Taiwan, China), performing a wash with demineralised water between each measurement, until reaching 0 °Brix. TA was measured by acid-base titration using 0.1 N NaOH and bromothymol blue as an indicator (Kontoudakis *et al.,* 2010). To obtain pH values, a portable pH meter (Extech, model 246072, Bogota, BTÁ, Colombia) was used, performing periodic calibrations between each treatment and repetition.

6. Reflectance spectrometry measurements

The spectral reflectance (SR) measurements of the berry samples were taken using a portable hyperspectral

spectroradiometer (HR-1024i, Spectra Vista Corporation, New York, NY, USA) connected to an optical fibre with a field of view (FOV) of 25°. The instrument can measure wavelengths between 350 and 2500 nm with intervals less or equal to 1.5, 3.8, and 2.5 nm in the range of 350–1000, 1000–1890, and 1890–2500 nm, respectively. Berries were placed on Petri dishes (9 cm in diameter) at 20 cm from the optical fibre. To measure SR, berries were exposed to direct light from halogen bulbs with a dichroic reflector inside a completely sealed black box. In this case, the dishes were used solely as a physical base to hold the berries, without being part of the active measurement area, so its influence on the spectral reflectance of the sample was negligible. Additionally, a reflective panel (white reference) (Spectralon, Panel, North Sutton, NH, USA) was placed between each measurement to obtain reference measurements at 100 % reflected light (Figure 1).

7. Optimisation of spectral information

A customised MATLAB code was developed by the Digital Agriculture group at Stellenbosch University (South Africa) to create contour maps that analyse the spectral information and associate it with the chemical variables measured at the laboratory. The code automatically resamples the spectra using a Savitzky–Golay filter that generates an interpolation process with a resolution of 1 nm, which is necessary for calculating narrow-band indices (Pôças *et al.,* 2015). Moreover, the code performs the matrix calculations of indices and correlations generating the contour maps associated with each variable.

8. Development of new spectral indices

Simple ratio indices (SR), which are defined as the quotient of the reflectances at two different wavelengths, highlight subtle variations in reflectance that might be difficult to discern in individual bands. The development of new indices was done using the contour map technique based on the principle of SR. This methodology involves testing various combinations of reflectance values within a given range VNIRS (350–2500 nm) with precision of 1 nm against a variable of interest through linear regressions. The result is a heat map where each pixel represents the determination coefficient (R^2) of a specific combination wavelength. Based on the above, the R^2 with the best value was adjusted to determine the optimised index that allows the variable in question to be better defined.

9. Development of models and validation

The development of linear models was through with season 2019/20 and validation was carried out by analysing the 2020/21 season by calculating the ratio of the estimated to observed values, root-mean-square error (RMSE), mean absolute error (MAE), and index of agreement (I_a) (Mayer & Butler, 1993; Willmott *et al.,* 1985).

$$RMSE = \left[N^{-1} \sum_{i=1}^{N} (P_i - O_i)^2\right]^{0,5} \quad (1)$$

$$MAE = N^{-1} \sum_{i=1}^{N} |P_i - O_i| \quad (2)$$

$$Ia = 1 - \left[\frac{\sum_{i=1}^{N} (P_i - O_i)^2}{\sum_{i=1}^{N} (|P_i - \bar{O}| + |O_i - \bar{O}|)^2}\right] \quad 0 \leq Ia \leq 1 \quad (3)$$

where N is the total number of observations, Pi and Oi are the estimated and observed values, respectively, and $\bar{O}$ is the mean of the observed values. In addition, the ratio of observed to estimated values was evaluated using the t-test at a 95 % confidence level.

Finally, ANOVA tests were conducted to determine the significant effect of irrigation treatments on SS, TA, and pH. In this case, Tukey's multiple comparison tests were used at 95 % confidence using RStudio (R: The R Project for Statistical Computing, 2023).

RESULTS

1. Measurements of stem water potential

The irrigation treatments resulted in a wide range of midday stem water potential (Ψx) values across the two seasons (Figure 2), ranging from –0.79 to –1.6 MPa in 2019/20 and from –0.65 to –1.50 MPa in 2020/21. These values indicate that the vines experienced water stress levels ranging from none to severe, based on the vine water deficit thresholds defined by van Leeuwen *et al.* (2009). Additionally, the irrigation treatments had a significant effect on nearly all analysed dates. In general, Ψx values were consistently higher in treatment T0 compared to T3. The most pronounced differences between these treatments were observed during the final week of January and the initial week of February. Subsequently, after irrigation restarted, Ψx values progressively increased across all treatments until harvest. At this phenological stage in the 2019/20 season, Ψx values in T3 were significantly higher than those in T0 and T2, which showed similar values. In contrast, during the 2020/21

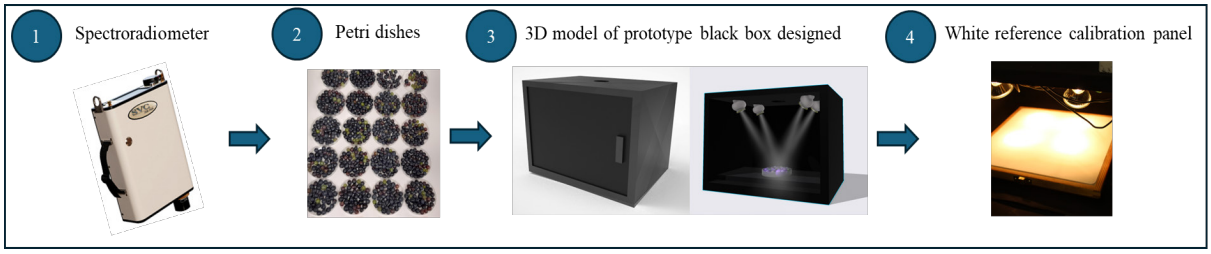


FIGURE 1. Reflectance spectral acquisition system.

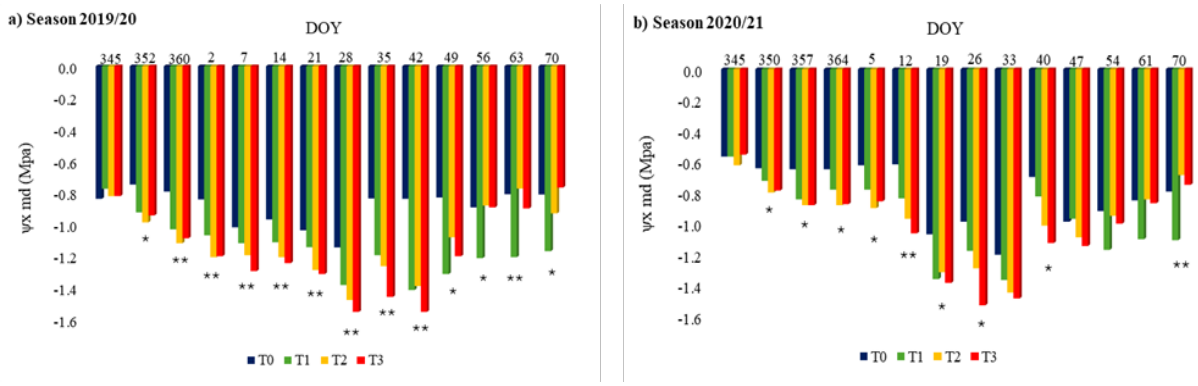


FIGURE 2. The daily evolution of midday stems water potential (Ψx) for grapevines (cv. Cabernet-Sauvignon) during the 2019/20 (a) and 2020/21 (b) growing seasons (Pencahue Valley, Maule, Chile). Treatments: T0 =100 % ETa from fruit set (FS) to harvest (H); T1 = 70 % from FS to H; ETa, T2 = 50 % ETa from FS to veraison (V) and 100 % ETa from V to H; T3 = 30 % ETa from FS to V and 100 % ETa from V to H.

season, T0, T2, and T3 presented comparable values, all of which were significantly higher than those of T1. The reason for this difference was that T1 was continuously maintained at only 70 % ETa replacement throughout the trial and never reached 100 % ETa.

2. Analysis and optimisation of spectral information

Based on spectral information obtained from Cabernet-Sauvignon under RDI in the 2019/20 and 2020/21 seasons considering all the treatments with different irrigation regimes, contour maps were generated in a wavelength range of 350–2500 nm with a 1 nm interval with respect to each of the variables individually: soluble solids, titratable acidity, and pH (Figure 3). The individualisation and optimisation of the wavelengths allowed for a more targeted analysis of all possible combinations within contour maps, facilitating the evaluation of their performance across both seasons. The maps display the coefficients of determination (R^2) between the maturity parameters and all possible combinations of two wavelengths, generated by a matrix that covers the entire spectral range along the horizontal (λx) and vertical (λy) axes. The results are visualised using a colour bar, where redder areas indicate wavelength combinations that produce stronger linear models with the maturity parameters. To identify common patterns across seasons for each maturity parameter, a visual selection criterion was applied. This process led to the identification of three common zones—also referred to as "hot spots" or clusters—where R^2 values were ≥ 0.8. These zones, highlighted with white squares, were recognised as consistent and persistent across seasons and were subsequently analysed individually.

Based on the above, the cluster patterns for soluble solids, titratable acidity, and pH showed similar trends across both measurement seasons: a small cluster in the VIS region (400–700 nm) (cluster 1), a more pronounced cluster in the NIR region (700–1200 nm) (cluster 2), and another in the SWIR region (1300–1700 nm) (cluster 3).

3. Development of new spectral indices

The analysis of each cluster allowed for the identification of the optimal wavelength combinations that produced the best linear models for each variable (Table 1). The best linear regressions were observed in cluster 3 with a spectral ratio of 1600 nm to 1412 nm (SI_{SS}) for soluble solids and 1617 to 1415 nm (SI_{TA}) for titratable acidity (TA), achieving R^2 values of 0.82 and 0.83, respectively. For pH, it was observed that cluster 1 produced the optimal linear model using a ratio of 694 nm to 697 nm (SI_{pH}), obtaining an R^2 of 0.95. Figure 4 shows the linear regression models using R1600/R1412, R1617/R1415, and R694/R697 ratios for predicting SS, TA, and pH, respectively, in grapevine under RDI treatments during the 2019/2020 growing season. In this case, the highest data dispersion was observed for SS between 22–25 °Brix (Figure 4a) and for TA between 3.5–7.5 g 100 mL^{-1} tartaric acid (Figure 4b), but the models presented a good performance. Figure 4c illustrates that the points for pH were close to the regression line. Finally, the

TABLE 1. Linear regression models for predicting soluble solids (SS), total acidity (TA), and pH based on new spectral indices (SI) in grapes under different levels of water application for the 2019/20 growing season. In addition, a and b represent the intercept and slope of the linear regression models, respectively.

Spectral Index	R^2	*a*	*b*
SI_{SS} = (R1600/R1412)	0.82	–184.99	211.54
SI_{TA} = (R1617/R1415)	0.83	258.28	–255.51
SI_{pH} = (R694/R697)	0.95	12.566	–8.22

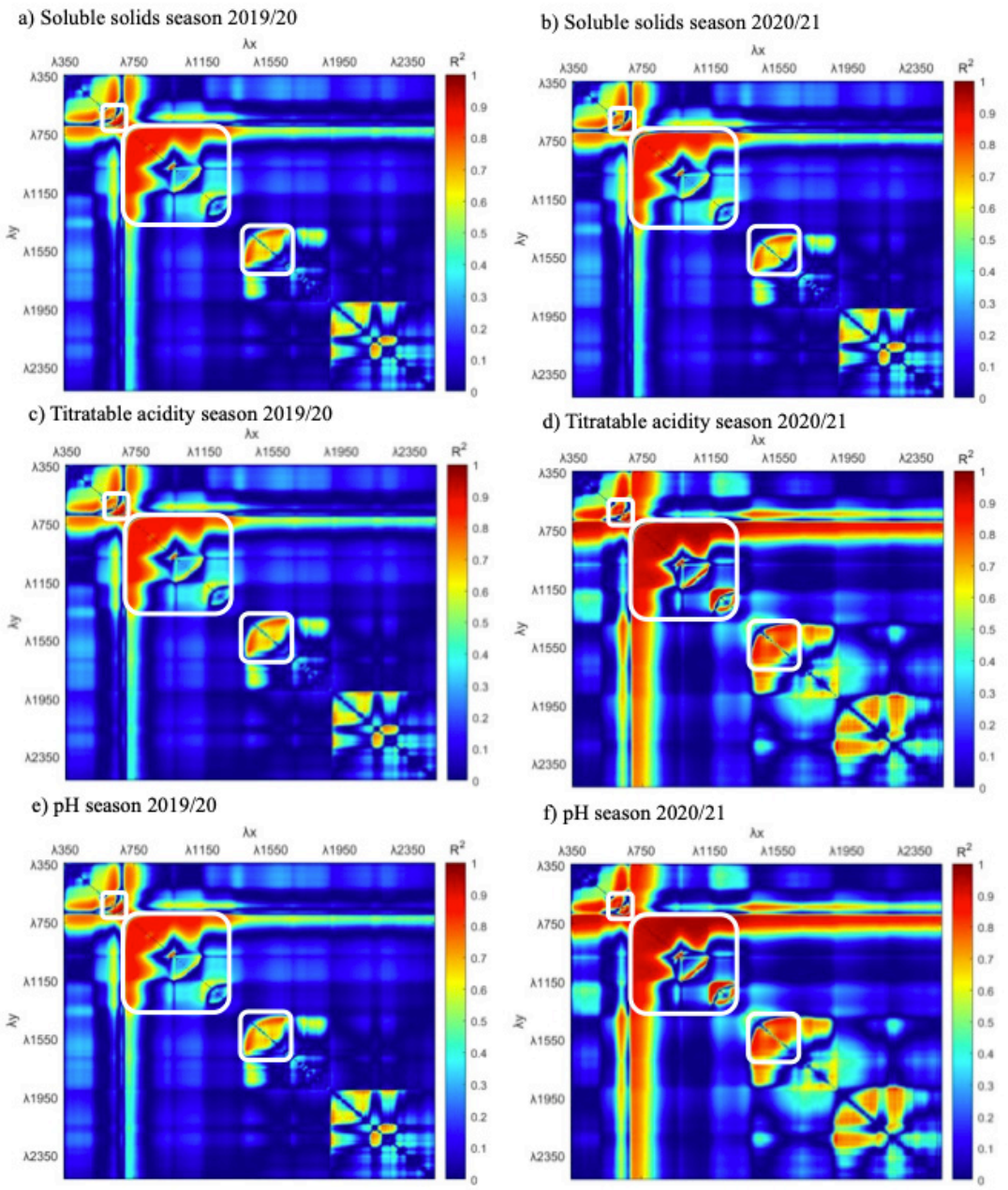


FIGURE 3. Contour maps for optimising the best linear correlation between spectral indices and quality parameters (soluble solids, titratable acidity, and pH) in grapes under different water levels during the 2019/20 and 2020/21 growing seasons.

performance of the three linear regression models was not affected by the RDI treatments suggesting that models based on simple ratios (**λx/λy**) can effectively monitor maturity in grape growing under different irrigation levels. This stability indicates that these models are consistent under varying irrigation regimes, making them valuable tools for assessing grapevine maturity, regardless of the water stress conditions.

The validation of linear regression models for predicting SS, TA, and pH based on the optimised spectral indices is indicated in Table 2. This table indicates that the I_a and R_{oe} values were between 0.79–0.94 and 0.93–1.05, respectively. The linear model based on SI_{ss} was the most accurate in estimating SS, with an RMSE of 1.15 °Brix and an MAE of 1.31 °Brix. In this case, the comparison plotted in Figure 5a shows that the points were very close to the 1:1 line with R_{oe} equal to unity at a 95 % confidence level. The worst agreement was found for the estimation of TA, with an RMSE of 1.60 g 100 mL^{-1} tartaric acid and an MAE of 2.28 g 100 mL^{-1} tartaric acid. A large dispersion of data points was observed, particularly for measured TA between 6–11 g 100 mL^{-1} tartaric acid (Figure 5b). In this case, R_{oe} was different from unity, suggesting that the SI_{TA}-based model underestimated the TA with an error of 7 %. Additionally, the linear regression model based on SI_{pH} overestimated the pH with errors of 5 %. In this case, main errors were observed for measured pH greater than 3.0 (Figure 5c).

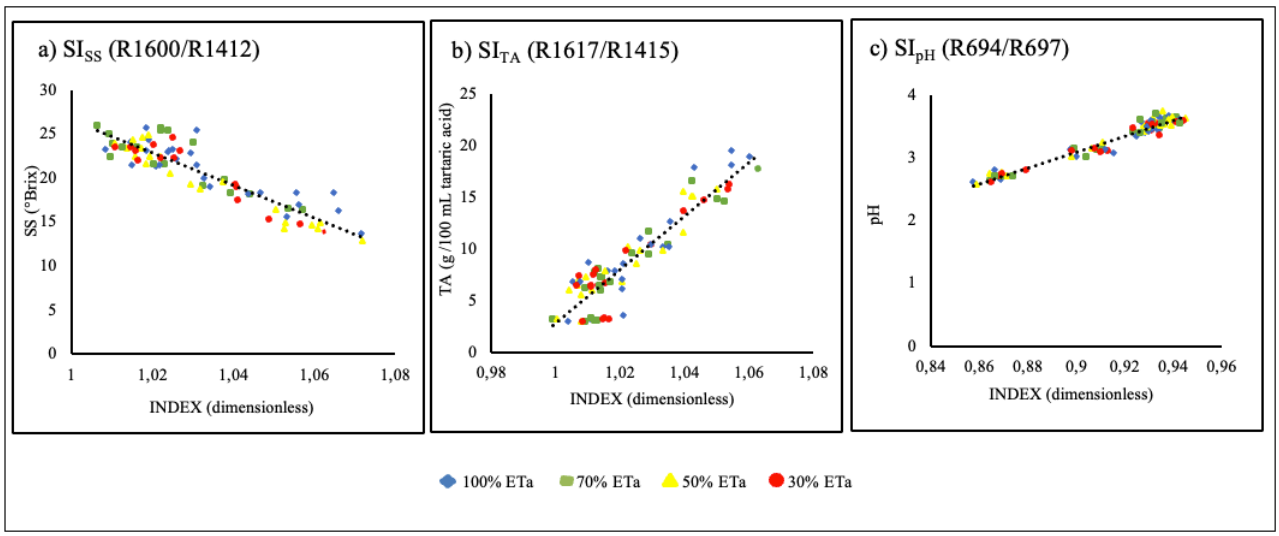


FIGURE 4. Linear regression models for predicting soluble solids (SS) (a), titratable acidity (TA) (b), and pH (c) based on spectral indices in grapes under different levels of water application for the 2019/20 growing season.

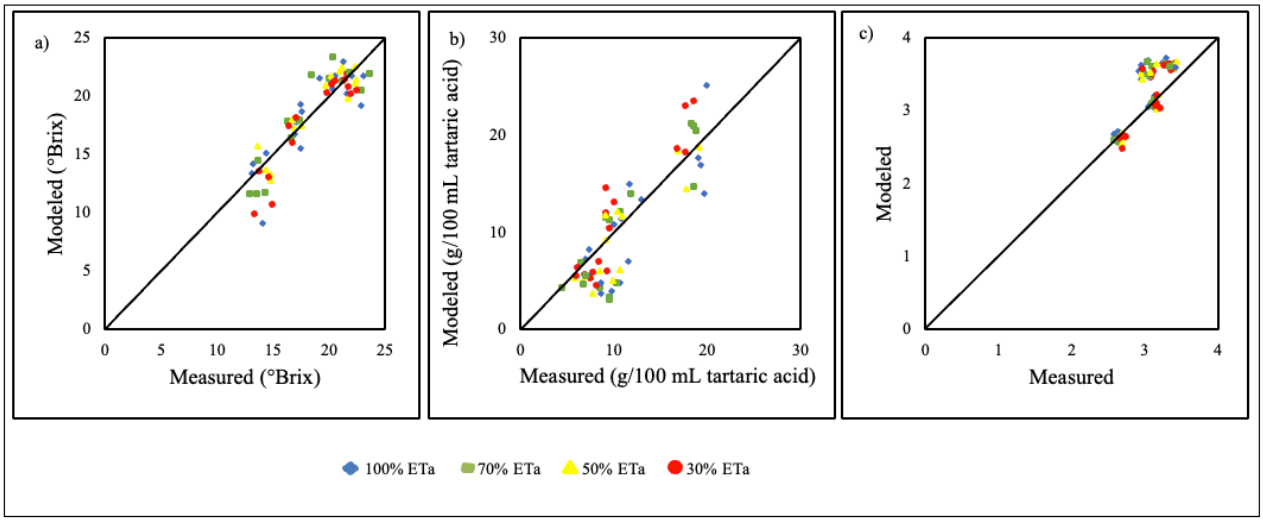


FIGURE 5. Comparison between modelled and measured values of soluble solids (SS) (a), total acidity (TA) (b), and pH (c) in grapes under different levels of water application for the 2020/21 growing season.

TABLE 2. Validation of linear regression models for predicting soluble solids (SS), total acidity, and pH based on spectral indices in grapes under different levels of water application for the 2020/21 growing season.

Spectral Index	RMSE	MAE	I_a	R_{oe}	*T*-test
SISS = (R1600/R1412)	1.15	1.31	0.94	1.01	T
SITA = (R1617/R1415)	1.60	2.28	0.90	0.93	F
SIpH = (R694/R697)	0.10	0.08	0.79	1.05	F

Where RMSE = root mean square error, MAE = mean absolute error, I_a = index of agreement, R_{oe} = ratio of observed to estimated values (*p*-value > 0.05), T null hypothesis (R_{oe} = 1) true, F alternative hypothesis ($R_{oe} \neq 1$) false.

The effect of four levels of water application on modelled and measured values of SS, TA, and pH in grapes are indicated in Table 3. This table indicates that the RDI treatments did not significantly affect the observed and estimated values of SS, TA, and pH for grape berries harvested from drip-irrigated vines under RDI. The measured values of SS, TA, and pH were between 21.9–24.4 °Brix, 6.4–7.5 g 100 mL^{-1} tartaric acid, and 3.3–3.4 for pH, respectively. While the estimated values were 20.7–21.4 °Brix, 5.0–6.4 g 100 mL^{-1} tartaric acid, and 3.6–3.7 pH units. Besides, neither the growing season nor the interaction between treatments and growing seasons had a significant effect.

TABLE 3. Effect of four levels of water application on observed and simulated values of soluble solids (SS), total acidity, and pH in grapes under different levels of water application for the 2020/21 growing season.

Treatment	SS (°Brix)		TA (g 100 mL^{-1} tartaric acid)		pH	
	Observed	Simulated	Observed	Simulated	Observed	Simulated
T0	22.4	20.7	7.5	6.4	3.3	3.7
T1	22.4	21.4	6.4	5.0	3.3	3.6
T2	22.3	21.0	6.4	5.9	3.4	3.6
T3	21.9	20.9	6.6	5.7	3.3	3.6
Significance	*n.s*	*n.s*	*n.s*	*n.s*	*n.s*	*n.s*

T0 =100 % of actual evapotranspiration (ETa); T1 = 70 % ETa; T2 = 50 % ETa between fruit set (FS) – veraison (V) and 100 % ETa between veraison - harvest; T3 = 30 % ETa between FS - V and 100 % ETa between V - H. Multiple comparisons in vertical direction when *n.s* = there were not significant differences ($p < 0.05$). For each treatment, values correspond to the average of four repetitions (200 berries/repetition).

DISCUSSION

The results indicate that the application of regulated deficit irrigation (RDI) did not have a significant effect on ripeness parameters at harvest (DOY 70). These findings are consistent with those reported by Wang *et al.* (2019) who evaluated different irrigation regimes and observed that, although RDI reduces vine vegetative growth, it did not significantly impact grape composition. This similarity may be attributed to the fact that, in both studies, irrigation was restored during the final stages, allowing the vines to recover from water stress and enabling proper berry ripening. In contrast, Munitz *et al.* (2020) reported significant differences in grape composition because sustained water deficit, maintained until harvest, continuously limited soil water availability to the vines.

This study determined that the application of the contour map methodology in the analysis of the full spectrum (350–2500 nm) allowed the identification of three spectral "hot spots". They were located in the ranges of 400–700 nm (cluster 1), 700–1200 nm (cluster 2), and 1300–1700 nm (cluster 3) and are sensitive to variations in SS, TA, and pH. These regions showed significant correlations with the ripeness parameters measured in this study ($R^2 > 0.8$ in most of the cases). This high level of correlation was consistent in both measurement seasons (2019/20 and 2020/21). From the clusters, the optimal linear regression models to simulate SS, TA, and pH were obtained using SI_{SS} (R1600/R1412), SI_{TA} (R1617/R1415), and SI_{pH} (R694/R697), respectively. The selection of these spectral indices was made using a specific statistical criterion, which allowed us to analyse the reliability of the results and adjust the most accurate models in terms of the maturity parameters.

Previous studies have reported that the VIS-NIR range enables the establishment of significant correlations with various maturity parameters in grapevines. For instance, Fadock *et al.* (2016) used the 350–800 nm spectrum to develop PLS models, achieving strong correlations (R^2 between 0.58 and 0.89) for the estimation of soluble solids and pH in Cabernet-Sauvignon, Cabernet franc, and Syrah. Similarly, Pampuri *et al.* (2022) analysed the 450–860 nm spectral range in grapevines cv. Chardonnay uses a Cost-Effective Visible/Near Infrared optical system, obtaining significant correlations for the estimation of the SS/TA ratio and pH. These findings support the suitability of the VIS-NIR range for the non-destructive determination of key maturity parameters in wine grapes.

Regarding the following "hot spots" which cover the spectral range from 700 to 1200 nm (cluster 2), it is visually the broadest category. Statistical analyses of the SI found in this area were performed to evaluate their estimation capability. However, the models developed in this spectral region did not show optimal performance and stability in both seasons. In contrast, Ferrara *et al.* (2022) reported high R^2 values for the prediction of ripening parameters (SS, TA, and pH) in Primitivo grapevines using a portable NIR device operating within the 740–1070 nm range, based on PLS analysis and various pre-processing methods. However, their models exhibited very high RMSE values, particularly for titratable acidity (TA), which exceeded 5.06 g/L.

Finally, in the 1300 to 1700 nm spectral range (cluster 3), the analysis identified well-defined "hot spots" associated with the highest statistical performance of the developed models, demonstrating strong correlations with the SS and TA. This region falls within the shortwave infrared (SWIR) domain, which is particularly sensitive to overtones and combination bands of molecular vibrations associated with carbohydrates, water, and organic acids-key components that undergo significant transformations during berry ripening (Mejía-Correal *et al.,* 2023; Siesler, 2016).

The relevance of this spectral range has been highlighted in previous studies, particularly by González-Caballero *et al.* (2010), who analysed the 380–1700 nm range and identified this region as crucial for the accurate prediction of SS, TA, and pH across different wine grape varieties using NIR-SWIR. Their results demonstrated high predictive accuracy, with R^2 values of 0.89 for SS, 0.87 for reducing sugars, and 0.69 for pH. This strong relationship is attributed to the interaction of these wavelengths with specific molecular vibrations linked to carbohydrate and water absorption, which are essential for the structural and biochemical modifications occurring in berries as sugar content increases and acidity

decreases. In agreement with these findings, the present study determined that the SWIR spectral region (1400–1600 nm) exhibited the strongest correlations for SS and TA estimation by using SI_{SS} (R^2 = 0.82) and SS_{TA} (R^2 = 0.83), respectively. Moreover, the consistency between both studies reinforces the applicability of NIRS in the non-destructive assessment of grape ripeness, enabling the implementation of field monitoring strategies and optimisation of decision-making in wineries.

In general, SR model stability over time and generalisation problems are largely attributed to high biological variability, which may be influenced by various factors such as cultivar, site-specific growing conditions, cultural practices, training systems, harvest season, and fruit ripening stages (Bedbabis *et al.,* 2014; Boselli *et al.,* 2019; Zheng *et al.,* 2020). The application of contour maps as a methodological tool addresses this issue by enabling the integration of a wide range of samples collected across different harvest periods (two or more seasons), including various developmental and ripening stages, thereby optimising model calibration.

The present study demonstrates that contour maps exhibit performance comparable to that of other methodologies based on advanced algorithms, such as Partial Least Squares Regression (PLSR), Random Forest Regression (RF), and Support Vector Regression (SVR). In this context, Kalopesa *et al.* (2023) developed predictive models using the full spectral range (350–2500 nm) to estimate soluble solids (SS), titratable acidity (TA), and pH in four wine grape varieties (Chardonnay, Malagouiza, Sauvignon blanc, and Syrah). The results indicated similar predictive performance for the different variables, with R^2 and RMSE varying depending on the variable analysed and the modelling phase. For SS, R^2 values ranged from 0.74 to 0.89 during model development, with an RMSE for °Brix between 1.39 and 1.91, while in validation, R^2 ranged from 0.64 to 0.85, with an RMSE between 1.44 and 2.36. For TA, R^2 values during modelling ranged from 0.67 to 0.83, with an RMSE between 2.06 and 2.85, whereas in validation, R^2 varied between 0.61 and 0.82, with an RMSE ranging from 1.66 to 2.22. Finally, for pH, the R^2 values during modelling ranged from 0.44 to 0.88, with an RMSE between 0.09 and 0.35, while in validation, R^2 fluctuated between 0.45 and 0.88, depending on the grape cultivar analysed.

Our study demonstrates the applicability of contour maps as an alternative method for extracting spectral features and identifying narrow and highly sensitive bands, which exhibit stable and specific performance in the estimation of various ripeness parameters. Our findings are consistent with prior research and support the usability of contour maps (Mariotto *et al.,* 2013; Rallo *et al.,* 2014; Yao *et al.,* 2010). The linear models based on new spectral indices obtained from contour maps confirmed their ability to monitor the evolution of maturity components from veraison to harvest (Gamboa *et al.,* 2024). Nevertheless, it is crucial to acknowledge that this method is susceptible to measurement noise and the presence of faulty sensors, which can result in inaccurate contour representations unless outliers are appropriately addressed (Meng *et al.,* 2006). Soil water availability affects the ability of reflectance indices to estimate quality attributes in vineyards (Rodríguez-Pérez *et al.,* 2022) and induces greater variability in the data, which could reflect the intrinsic variability present under field conditions. In this regard, further research is needed to evaluate the effectiveness of these models in different grape varieties and growing conditions, as well as to develop more reliable models for predicting the important maturity components of grapes.

A future direction for this research involves adapting the developed spectral indices for use in more accessible field-based systems. Specifically, evaluating the integration of these indices into low-cost sensors operating within the identified relevant spectral regions would be valuable. This could lead to the development of portable or ground-based devices for direct cluster-level measurements in practical vineyard conditions, advancing non-destructive monitoring tools in viticulture.

CONCLUSION

This study demonstrated that the optimisation of spectral indices through contour mapping significantly improves the accuracy and stability of non-destructive grape ripeness assessment. By analysing hyperspectral reflectance data (350–2500 nm), three optimal wavelength combinations were identified, enabling the development of robust spectral indices for predicting soluble solids, titratable acidity, and pH. Validation of these models in an independent season confirmed their stability under variable water availability conditions, suggesting their applicability across different production environments. The use of contour mapping not only optimised the selection of key wavelengths but also reduced the dependence on site-specific calibrations, increasing the generalisation capacity of the developed spectral indices. Finally, the application of contour mapping in the development of spectral indices constitutes a significant methodological advancement for non-destructive grape ripeness assessment.

ACKNOWLEDGEMENTS

This study was supported by the Chilean government through the projects FONDEQUIP (EQU-009CONICYT) and FONDECYT (Nº 1230500). The authors would like to thank Dr Alvaro Gonzalez ("Viña Concha y Toro" winery) for allowing us to set up the trials in the company´s vineyards. Also, to Scholarship to promote the internationalisation of master's degree programs, R.U. Nº 136/2019 by the University of Talca, Chile.

REFERENCES

Basile, T., Marsico, A. D., & Perniola, R. (2021). NIR Analysis of Intact Grape Berries: Chemical and Physical Properties Prediction Using Multivariate Analysis. Foods 2021, Vol. 10, Page 113, 10(1), 113. https://doi.org/10.3390/FOODS10010113

Bedbabis, S., Ben Rouina, B., Boukhris, M., & Ferrara, G. (2014). Effects of Irrigation with Treated Wastewater on Root and Fruit Mineral Elements of Chemlali Olive Cultivar. The Scientific World Journal, 2014(1), 973638. https://doi.org/10.1155/2014/973638

Boselli, M., Bahouaoui, M. A., Lachhab, N., Sanzani, S. M., Ferrara, G., & Ippolito, A. (2019). Protein hydrolysates effects on grapevine (Vitis vinifera L., cv. Corvina) performance and water stress tolerance. Scientia Horticulturae, 258, 108784. https://doi.org/10.1016/J.SCIENTA.2019.108784

Cao, F., Xie, X., Gollan, T., Zhao, L., Narsinh, K., Lee, R. J., & Wu, J. C. (2010). Comparison of gene-transfer efficiency in human embryonic stem cells. Molecular Imaging and Biology, 12(1), 15–24. https://doi.org/10.1007/S11307-009-0236-X/FIGURES/5

Chariskou, C., Vrochidou, E., Daniels, A. J., & Kaburlasos, V. G. (2022). Variable Selection on Reflectance NIR Spectra for the Prediction of TSS in Intact Berries of Thompson Seedless Grapes. Agronomy, 12(9), 2113. https://doi.org/10.3390/AGRONOMY12092113/S1

Costa, G., Noferini, M., Fiori, G., & Torrigiani, P. (2022). Use of Vis/NIR Spectroscopy to Assess Fruit Ripening Stage and Improve Management in Post-Harvest Cha. FRESH PRODUCE, 3(special issue 1), 35–41. https://cris.unibo.it/handle/11585/81868

Daniels, A. J., Poblete-Echeverría, C., Opara, U. L., & Nieuwoudt, H. H. (2019). Measuring Internal Maturity Parameters Contactless on Intact Table Grape Bunches Using NIR Spectroscopy. Frontiers in Plant Science, 10, 480410. https://doi.org/10.3389/FPLS.2019.01517/BIBTEX

del Pozo, A., Brunel-Saldias, N., Engler, A., Ortega-Farias, S., Acevedo-Opazo, C., Lobos, G. A., Jara-Rojas, R., & Molina-Montenegro, M. A. (2019). Climate Change Impacts and Adaptation Strategies of Agriculture in Mediterranean-Climate Regions (MCRs). Sustainability 2019, Vol. 11, Page 2769, 11(10), 2769. https://doi.org/10.3390/SU11102769

Donis-González, I. R., Valero, C., Momin, M. A., Kaur, A., & Slaughter, D. C. (2020). Performance Evaluation of Two Commercially Available Portable Spectrometers to Non-Invasively Determine Table Grape and Peach Quality Attributes. Agronomy 2020, Vol. 10, Page 148, 10(1), 148. https://doi.org/10.3390/AGRONOMY10010148

Fadock, M., Brown, R. B., & Reynolds, A. G. (2016). Visible-near infrared reflectance spectroscopy for nondestructive analysis of red wine grapes. American Journal of Enology and Viticulture, 67(1), 38–45. https://doi.org/10.5344/AJEV.2015.15035

Fernandes, A. M., Franco, C., Mendes-Ferreira, A., Mendes-Faia, A., Costa, P. L. da, & Melo-Pinto, P. (2015). Brix, pH and anthocyanin content determination in whole Port wine grape berries by hyperspectral imaging and neural networks. Computers and Electronics in Agriculture, 115, 88–96. https://doi.org/10.1016/J.COMPAG.2015.05.013

Fernández-Novales, J., Tardáguila, J., Gutiérrez, S., & Paz Diago, M. (2019). On-The-Go VIS + SW ? NIR Spectroscopy as a Reliable Monitoring Tool for Grape Composition within the Vineyard. Molecules 2019, Vol. 24, Page 2795, 24(15), 2795. https://doi.org/10.3390/MOLECULES24152795

Fulton, A., Grant, J., Buchner, R., & Connell, J. (2014). Using the Pressure Chamber for Irrigation Management in Walnut, Almond and Prune. In Using the Pressure Chamber for Irrigation Management in Walnut, Almond and Prune. https://doi.org/10.3733/ucanr.8503

Ferrara, G., Melle, A., Marcotuli, V., Botturi, D., Fawole, O. A., & Mazzeo, A. (2022). The prediction of ripening parameters in Primitivo wine grape cultivar using a portable NIR device. Journal of Food Composition and Analysis, 114, 104836. https://doi.org/10.1016/J.JFCA.2022.104836

Gambetta, G. A., Herrera, J. C., Dayer, S., Feng, Q., Hochberg, U., & Castellarin, S. D. (2020). The physiology of drought stress in grapevine: towards an integrative definition of drought tolerance. Journal of Experimental Botany, 71(16), 4658. https://doi.org/10.1093/JXB/ERAA245

Gamboa, M. J., Ortega-Farias, S., de la Fuente, D., Fuentes-Peñailillo, F., Vargas, S., & Laurie, V. F. (2024). Grape ripening and phenolic content monitoring in Cabernet-Sauvignon under regulated deficit irrigation using spectral reflectance indices. Scientia Horticulturae, 328, 112920. https://doi.org/10.1016/J.SCIENTA.2024.112920

Ghozlen, N. Ben, Cerovic, Z. G., Germain, C., Toutain, S., & Latouche, G. (2010). Non-Destructive Optical Monitoring of Grape Maturation by Proximal Sensing. Sensors 2010, Vol. 10, Pages 10040-10068, 10(11), 10040–10068. https://doi.org/10.3390/S101110040

Giovenzana, V., Beghi, R., Mena, A., Civelli, R., Guidetti, R., Best, S., & Leòn Gutiérrez, L. F. (2013). Quick quality evaluation of Chilean grapes by a portable vis/NIR device. Acta Horticulturae, 978, 93–100. https://doi.org/10.17660/ACTAHORTIC.2013.978.9

Goisser, S., Wittmann, S., & Mempel, H. (2021). Anwendungen von Food-Scannern im Obst- und Gemüsesektor. Agricultural Engineering. Eu, 76(1), 52–67. https://doi.org/10.15150/LT.2021.3264

González-Caballero, V., Sánchez, M. T., López, M. I., & Pérez-Marín, D. (2010). First steps towards the development of a non-destructive technique for the quality control of wine grapes during on-vine ripening and on arrival at the winery. Journal of Food Engineering, 101(2), 158–165. https://doi.org/10.1016/J.JFOODENG.2010.06.016

Inoue, Y., Peñuelas, J., Miyata, A., & Mano, M. (2008). Normalized difference spectral indices for estimating photosynthetic efficiency and capacity at a canopy scale derived from hyperspectral and CO2 flux measurements in rice. Remote Sensing of Environment, 112(1), 156–172. https://doi.org/10.1016/J.RSE.2007.04.011

Jara Rojas, F., Ortega Farias, S. O., Valdés Gómez, H., & Acevedo Opazo, C. (2015). Gas exchange relations of ungrafted grapevines (cv. Carménère) growing under irrigated field conditions. South African Journal of Enology and Viticulture, ISSN 0253-939X, Vol. 36, No 2, 2015, Págs. 231-242, 36(2), 231–242. https://dialnet.unirioja.es/servlet/articulo?codigo=5215248

Kalopesa, E., Gkrimpizis, T., Samarinas, N., Tsakiridis, N. L., & Zalidis, G. C. (2023). Rapid Determination of Wine Grape Maturity Level from pH, Titratable Acidity, and Sugar Content Using Non-Destructive In Situ Infrared Spectroscopy and Multi-Head Attention Convolutional Neural Networks. Sensors 2023, Vol. 23, Page 9536, 23(23), 9536. https://doi.org/10.3390/S23239536

Kemps, B., Leon, L., Best, S., De Baerdemaeker, J., & De Ketelaere, B. (2010). Assessment of the quality parameters in grapes using VIS/NIR spectroscopy. Biosystems Engineering, 105(4), 507–513. https://doi.org/10.1016/J.BIOSYSTEMSENG.2010.02.002

Kontoudakis, N., Esteruelas, M., Fort, F., Canals, J. M., & Zamora, F. (2010). Comparison of methods for estimating phenolic maturity in grapes: Correlation between predicted and obtained parameters. Analytica Chimica Acta, 660(1–2), 127–133. https://doi.org/10.1016/J.ACA.2009.10.067

Macedo, A., Gouveia, S., Rebelo, J., Santos, J., & Fraga, H. (2020). International trade, non-tariff measures and climate change: insights from Port wine exports. Journal of Economic Studies, 48(6), 1228–1243. https://doi.org/10.1108/JES-04-2020-0161/FULL/PDF

Manley, M. (2014). Near-infrared spectroscopy and hyperspectral imaging: non-destructive analysis of biological materials. Chemical Society Reviews, 43(24), 8200–8214. https://doi.org/10.1039/C4CS00062E

Mariotto, I., Thenkabail, P. S., Huete, A., Slonecker, E. T., & Platonov, A. (2013). Hyperspectral versus multispectral crop-productivity modeling and type discrimination for the HyspIRI mission. Remote Sensing of Environment, 139, 291–305. https://doi.org/10.1016/J.RSE.2013.08.002

Mayer, D. G., & Butler, D. G. (1993). Statistical validation. Ecological Modelling, 68(1–2), 21–32. https://doi.org/10.1016/0304-3800(93)90105-2

Mejía-Correal, K. B., Marcelo, V., Sanz-Ablanedo, E., & Rodríguez-Pérez, J. R. (2023). Total Soluble Solids in Grape Must Estimation Using VIS-NIR-SWIR Reflectance Measured in Fresh Berries. Agronomy, 13(9), 2275. https://doi.org/10.3390/AGRONOMY13092275/S1

Meng, X., Nandagopal, T., Li, L., & Lu, S. (2006). Contour maps: Monitoring and diagnosis in sensor networks. Computer Networks, 50(15), 2820–2838. https://doi.org/10.1016/j.comnet.2005.09.038

Munitz, S., Schwartz, A., & Netzer, Y. (2020). Effect of timing of irrigation initiation on vegetative growth, physiology and yield parameters in Cabernet Sauvignon grapevines. In Australian Journal of Grape and Wine Research (Vol. 26, Issue 3, pp. 220–232). John Wiley & Sons, Ltd. https://doi.org/10.1111/ajgw.12435

Ortega-Farias, S., Fereres, E., & Sadras, V. O. (2012). Special issue on water management in grapevines. Irrigation Science, 30(5), 335–337. https://doi.org/10.1007/S00271-012-0356-Y/METRICS

OIV. (2025). Compendium of International Methods of Analysis for Vinegars. International Organisation of Vine and Wine. https://www.oiv.int/es/standards/compendium-of-international-methods-of-analysis-for-vinegars

Pampuri, A., Tugnolo, A., Giovenzana, V., Casson, A., Pozzoli, C., Brancadoro, L., Guidetti, R., & Beghi, R. (2022). Application of a Cost-Effective Visible/Near Infrared Optical Prototype for the Measurement of Qualitative Parameters of Chardonnay Grapes. Applied Sciences 2022, Vol. 12, Page 4853, 12(10), 4853. https://doi.org/10.3390/APP12104853

Piazzolla, F., Amodio, M. L., & Colelli, G. (2013). The use of hyperspectral imaging in the visible and near infrared region to discriminate between table grapes harvested at different times. Journal of Agricultural Engineering, 44(2), e7–e7. https://doi.org/10.4081/JAE.2013.E7

Pôças, I., Rodrigues, A., Gonçalves, S., Costa, P. M., Gonçalves, I., Pereira, L. S., & Cunha, M. (2015). Predicting Grapevine Water Status Based on Hyperspectral Reflectance Vegetation Indices. Remote Sensing 2015, Vol. 7, Pages 16460-16479, 7(12), 16460–16479. https://doi.org/10.3390/RS71215835

R: The R Project for Statistical Computing. (2023). https://www.r-project.org/

Rallo, G., Minacapilli, M., Ciraolo, G., & Provenzano, G. (2014). Detecting crop water status in mature olive groves using vegetation spectral measurements. Biosystems Engineering, 128, 52–68. https://doi.org/10.1016/J.BIOSYSTEMSENG.2014.08.012

Ribera-Fonseca, A., Noferini, M., Jorquera-Fontena, E., & Rombolà, A. D. (2016). Assessment of technological maturity parameters and anthocyanins in berries of cv. Sangiovese (Vitis vinifera L.) by a portable vis/NIR device. Scientia Horticulturae, 209, 229–235. https://doi.org/10.1016/J.SCIENTA.2016.06.004

Rodríguez-Pérez, R., Agugliaro, F. M., Serrano, L., & Gorchs, G. (2022). Water Availability Affects the Capability of Reflectance Indices to Estimate Berry Yield and Quality Attributes in Rain-Fed Vineyards. Agronomy 2022, Vol. 12, Page 2091, 12(9), 2091. https://doi.org/10.3390/AGRONOMY12092091

Rouxinol, M. I., Martins, M. R., Murta, G. C., Barroso, J. M., & Rato, A. E. (2022). Quality Assessment of Red Wine Grapes through NIR Spectroscopy. Agronomy, 12(3), 637. https://doi.org/10.3390/AGRONOMY12030637/S1

Santos, J. A., Fraga, H., Malheiro, A. C., Moutinho-Pereira, J., Dinis, L. T., Correia, C., Moriondo, M., Leolini, L., Dibari, C., Costafreda-Aumedes, S., Kartschall, T., Menz, C., Molitor, D., Junk, J., Beyer, M., & Schultz, H. R. (2020). A Review of the Potential Climate Change Impacts and Adaptation Options for European Viticulture. Applied Sciences 2020, Vol. 10, Page 3092, 10(9), 3092. https://doi.org/10.3390/APP10093092

Scholander, P. F., Bradstreet, E. D., Hemmingsen, E. A., & Hammel, H. T. (1965). Sap Pressure in Vascular Plants: Negative hydrostatic pressure can be measured in plants. Science (New York, N.Y.), 148(3668). https://doi.org/10.1126/science.148.3668.339

Siesler, H. W. (2016). Vibrational Spectroscopy. Reference Module in Materials Science and Materials Engineering. https://doi.org/10.1016/B978-0-12-803581-8.01318-7

Suarez, L., Zhang, P., Sun, J., Wang, Y., Poblete, T., Hornero, A., & Zarco-Tejada, P. J. (2021). Assessing wine grape quality parameters using plant traits derived from physical model inversion of hyperspectral imagery. Agricultural and Forest Meteorology, 306, 108445. https://doi.org/10.1016/J.AGRFORMET.2021.108445

Tardaguila, J., Stoll, M., Gutiérrez, S., Proffitt, T., & Diago, M. P. (2021). Smart applications and digital technologies in viticulture: A review. Smart Agricultural Technology, 1, 100005. https://doi.org/10.1016/J.ATECH.2021.100005

Tian, Y. C., Yao, X., Yang, J., Cao, W. X., Hannaway, D. B., & Zhu, Y. (2011). Assessing newly developed and published vegetation indices for estimating rice leaf nitrogen concentration with ground- and space-based hyperspectral reflectance. Field Crops Research, 120(2), 299–310. https://doi.org/10.1016/J.FCR.2010.11.002

van Leeuwen, C., Tregoat, O., Choné, X., Bois, B., Pernet, D., & Gaudillére, J. P. (2009). Vine water status is a key factor in grape ripening and vintage quality for red Bordeaux wine. How can it be assessed for vineyard management purposes? OENO One, 43(3), 121–134. https://doi.org/10.20870/OENO-ONE.2009.43.3.798

Walsh, K. B., Blasco, J., Zude-Sasse, M., & Sun, X. (2020). Visible-NIR 'point' spectroscopy in postharvest fruit and vegetable assessment: The science behind three decades of commercial use. Postharvest Biology and Technology, 168, 111246. https://doi.org/10.1016/J.POSTHARVBIO.2020.111246

Wang, R., Yan, P., Sun, Q., Su, B., & Zhang, J. (2019). Effects of regulated deficit irrigation on the growth and berry composition of Cabernet sauvignon in Ningxia. International Journal of Agricultural and Biological Engineering, 12(6), 102–109. https://doi.org/10.25165/j.ijabe.20191206.5206

Willmott, C. J., Ackleson, S. G., Davis, R. E., Feddema, J. J., Klink, K. M., Legates, D. R., O'Donnell, J., & Rowe, C. M. (1985). Statistics for the evaluation and comparison of models. Journal of Geophysical Research: Oceans, 90(C5), 8995–9005. https://doi.org/10.1029/JC090IC05P08995

Yao, X., Zhu, Y., Tian, Y. C., Feng, W., & Cao, W. X. (2010). Exploring hyperspectral bands and estimation indices for leaf nitrogen accumulation in wheat. International Journal of Applied Earth Observation and Geoinformation, 12(2), 89–100. https://doi.org/10.1016/J.JAG.2009.11.008

Zheng, W., Bai, Y., Luo, H., Li, Y., Yang, X., & Zhang, B. (2020). Self-adaptive models for predicting soluble solid content of blueberries with biological variability by using near-infrared spectroscopy and chemometrics. Postharvest Biology and Technology, 169, 111286. https://doi.org/10.1016/J.POSTHARVBIO.2020.111286

Zúñiga, M., Ortega-Farías, S., Fuentes, S., Riveros-Burgos, C., & Poblete-Echeverría, C. (2018). Effects of three irrigation strategies on gas exchange relationships, plant water status, yield components and water productivity on grafted carménère grapevines. Frontiers in Plant Science, 9, 370767. https://doi.org/10.3389/FPLS.2018.00992/BIBTEXÂ